

LASER APPLICATIONS AND OTHER TOPICS IN QUANTUM ELECTRONICS

PACS numbers: 78.20.Ci; 61.72.y; 42.70.Mp
DOI: 10.1070/QE2000v030n08ABEH001799

Influence of structural defects on the optical properties of Mg : $LiNbO_3$ single crystals

G Kh Kitaeva, K A Kuznetsov, I I Naumova, A N Penin

Abstract. A comparative analysis of the dependences of the refractive index of Mg:$LiNbO_3$ single crystals on the Mg concentration is performed in the visible and IR transparency regions. The results of measurements at the wavelengths above 4 μm suggest the four-step mechanism of incorporation of the Mg impurity to the $LiNbO_3$ crystal in the range of molar concentrations of Mg from 0 to 7.1 %. The resonances observed between 1 and 2 μm and between 2.8 and 3.5 μm in the transparency region are interpreted as contributions from polaron states. It is shown that the resonance in the region between 1 and 2 μm is strongly enhanced in crystals with the molar concentration of Mg above 5.1 %.

1. Introduction

The uniqueness of a $LiNbO_3$ crystal is universally known. It attracts the attention of researchers in quite diverse, often unrelated studies in the fields of nonlinear optics, quantum electronics, and solid-state physics. This crystal is still one of the best materials for the laser radiation frequency conversion (owing to its high nonlinear susceptibility and the possibility to obtain quasi-phase-matching conditions [1]), it is used in electro-optics [2], is promising for data storage [3], etc.

Even nominally pure $LiNbO_3$ crystals differ in their chemical composition (the ratio of the number of lithium atoms to that of the niobium atoms $R \equiv [\mathrm{Li}]/[\mathrm{Nb}]$ can vary from 0.8 to 1.0 and more), resulting in a high concentration of defects of various types [4, 5]. In addition, nominally pure crystals possess photorefractive properties which cause a strong change in optical characteristics upon exposure to high-power laser radiation, and to suppress the photorefraction, some chemical elements, for example, Mg, Sc, Zn, or In [6] are added as impurities in melts from which the crystals are grown. On the other hand, the use of the such impurities as Fe and Cu enhance photorefraction [7]. The interaction of impurities with intrinsic defects makes the structure of real crystals extremely complex, and the specific shape of the dispersion dependences of optical parameters is virtually unpredictable.

G Kh Kitaeva, K A Kuznetsov, I I Naumova, A N Penin Department of Physics, M V Lomonosov Moscow State University, Vorob'evy gory, 119899 Moscow, Russia

Received 20 January 2000
Kvantovaya Elektronika **30** (8) 726 – 732 (2000)
Translated by M N Sapozhnikov

As a rule, the studies of dispersion parameters of lithium niobate crystals have been performed in the visible spectral region [8]. The aim of this paper is to study the dispersion of the refractive index of Mg : $LiNbO_3$ crystals over the entire transparency region. In addition to obvious practical applications, for example, for calculation of phase-matching conditions under frequency conversion in a broad frequency range, the data obtained yield information on the dynamics of variation in the structural defects with increasing doping degree.

2. Experiment

2.1. Samples

The Mg:$LiNbO_3$ single crystals were grown by the Czochralski method from a melt of a composition close to a congruent one ($R = 0.942$). The molar concentration of the MgO impurity was varied from 0 to $\sim 7\,\%$. The concentration of magnesium in crystals was measured by the methods of dispersion x-ray microanalysis and fluorescence x-ray spectral analysis. The relative measurements showed that the inhomogeneity of the impurity concentration distribution over the sample volume was $\pm 0.01 - 0.03\,\%$. However, the absolute measurement error of the impurity concentration C_{Mg} averaged over the sample volume was substantially larger and amounted to $\pm 0.4\,\%$ for some crystals.

2.2. Measurements of n_o and n_e in the visible region

We measured the refractive indices n_o and n_e for ordinary and extraordinary polarised waves in the visible spectral range by the method of minimum prism deviation angle using a G-5 goniometer. The absolute measurement error of the refractive index was about $\pm 2 \times 10^{-4}$. Table 1 presents the results of measurements of n_o and n_e at different wavelengths, and Table 2 lists the Sellmeyer constants A, B, C, and D. The refractive indices calculated by the Sellmeyer formulas

$$n_{o,e}^2 = A_{o,e} - \frac{B_{o,e}}{C_{o,e} - \lambda^2} - D_{o,e}\lambda^2, \qquad (1)$$

where λ is the wavelength in nanometers, differ from measured refractive indices less than by $\pm 4 \times 10^{-4}$.

2.3. Measurement of n_o in the range between 1.06 and 1.25 μm

Dispersion of the refractive index of the crystals in the near-IR region was measured using the 1.06-μm Nd : YAG laser

Table 1. Measured refractive indices n_o and n_e.

Wavelength/nm	Polarisation	Molar concentration of the Mg impurity (%				
		0	4.4±0.1	5.1±0.1*	6.1±0.2*	7.1±0.2
435.8	o	2.3931	2.3876	2.3863	2.3812	2.3786
	e	2.2926	2.2786	2.2802	2.2795	2.2789
476.5	o	2.3575	–	2.3506	2.3457	2.3434
	e	2.2626	–	2.2503	2.2492	2.2494
488	o	2.349	–	2.3426	2.3377	2.3353
	e	2.2554	–	2.2436	2.2424	2.2426
496.5	o	2.3434	–	2.3371	2.3322	2.3298
	e	2.2508	–	2.239	2.2378	2.238
501.7	o	2.3401	–	2.3339	2.3291	2.3268
	e	2.2478	–	2.2363	2.2351	2.2354
532	o	2.3238	–	2.3176	2.3129	2.3105
	e	2.2338	–	2.2226	2.2214	2.2217
546.1	o	2.3167	2.3124	2.3111	2.3065	2.3041
	e	2.2278	2.2161	2.2172	2.2161	2.2161
577	o	2.3042	2.2992	2.2989	2.2943	2.2918
	e	2.2171	2.2056	2.2068	2.2057	2.2057
579	o	2.3034	2.2987	2.2982	2.2936	2.2911
	e	2.2165	2.205	2.2062	2.2051	2.205
632.8	o	2.2872	2.2821	2.2817	2.2772	2.2748
	e	2.2028	2.1909	2.1922	2.1914	2.1909
1064	o	2.2319	–	2.2276	2.2237	–
	e	2.1539	–	2.1463	2.1458	–

*These data have been already presented by us [9]; however, then only the MgO impurity concentration in initial melts was known.

Table 2. Measured Sellmeyer constants A, B, C, D.

Molar concentration of the Mg impurity (%)	Polarisation	A	$B/10^4$	$C/10^4$	$D/10^{-8}$
0	o	5.1119	7.9785	7.2039	31.814
	e	4.6622	8.3052	5.6072	13.468
4.4 ± 0.1	o	4.8613	12.4489	4.1701	0.26404
	e	4.5176	10.2295	3.8244	3.446×10^{-5}
5.1 ± 0.1	o	4.9017	11.228	4.9656	3.9636
	e	4.5562	9.2477	4.7392	3.0468
5.7 ± 0.4	o	4.8653	12.1942	3.9672	2.2469
	e	4.5777	8.5685	5.2882	4.5927
6.1 ± 0.2	o	4.8853	11.0339	5.0611	3.7461
	e	4.5667	8.7092	5.3129	3.7905
7.1 ± 0.2	o	4.8452	11.754	4.5396	0.44963
	e	4.5401	9.6132	4.3931	2.3567

and a tunable F_2^- : LiF laser operating at 1.133 and 1.246 μm. Using the relations, which follow from the spatial phase-matching conditions for the interaction of the ooe type, we measured the angle between the input face plane and optical axis of each rectangular sample, the phase-matching angle, and ordinary refractive indices $n_o(\lambda)$ at the pump waves. The refractive indices $n_o(\lambda/2)$ and $n_e(\lambda/2)$ were calculated by Sellmeyer formulas (1) in the visible range.

Table 3 presents the values of n_o measured with an accuracy of $\pm 5 \times 10^{-4}$. In crystals with the magnesium concentration equal to 5.1 and 6.1 %, n_o was also measured at 1.064 μm by the prism method (Table 1). The results of measurements by these two methods are in good agreement within the net accuracy.

Table 3. Measured refractive indices n_o.

Wavelength/nm	Polarisation	Molar concentration of the Mg impurity (%)					
		0	4.4±0.1	5.1±0.1	5.7±0.4	6.1±0.2	7.1±0.2
1064	o	–	2.2281	2.2277	2.2250	2.2231	2.2222
1133.4	o	2.229	2.2244	2.2238	2.2216	2.2193	2.2183
1246	o	2.2206	–	–	–	–	–

2.4. Measurement of n_o in the range between 2 and 5 μm

The dispersion dependences of the crystals in a longer-wavelength spectral region (Table 4) were measured by a standard method of spontaneous parametric light scattering described, for example, in Ref. [10]. Pumping was performed by a 500-mW 488-nm line from an argon laser. The error of measurement of n_o in the spectral range between 2 and 5 μm varied from $\pm 5 \times 10^{-4}$ to $\pm 2 \times 10^{-3}$, increasing with the wavelength of measurements.

Table 4. Measured refractive indices n_o.

Wavelength/nm	Polarisation	Molar concentration of the Mg impurity (%)					
		0	4.4±0.1	5.1±0.1	5.7±0.4	6.1±0.2	7.1±0.2
2.124	o	2.1937	2.1910	2.1841	2.1805	2.1798	2.1810
2.241	o	2.1869	2.1831	2.1807	2.1769	2.1752	2.1769
2.348	o	2.1825	2.1827	2.1772	2.1732	2.1713	2.1737
2.596	o	2.1710	2.1731	2.1659	2.1619	2.1625	2.1627
2.802	o	2.1593	2.1643	2.1582	2.1545	2.1525	2.1534
3.050	o	2.1471	2.1482	2.1482	2.1423	2.1413	2.1409
3.359	o	2.1341	2.1335	2.1336	2.1265	2.1244	2.1269
3.759	o	2.1097	2.1158	2.1127	2.1061	2.1013	2.1053
4.296	o	2.069	2.074	2.078	2.070	2.065	2.069
4.927	o	2.018	2.018	2.033	2.018	2.010	2.015

3. Analysis of concentration dependences

We will analyse the influence of a dopant on the optical properties of $Mg:LiNbO_3$ using the difference method, which possesses a higher sensitivity to small variations in the quantities measured. The difference $\delta_{o,e}(C_{Mg},\lambda) \equiv n^2_{o,e}(C_{Mg},\lambda) - n^2_{o,e}(0,\lambda)$ in the transparency region of crystals characterise the difference between real parts of the permittivity of doped and nominally pure crystals. Even quite a small variation in the spectral dependences of $n_{o,e}$ caused by doping (a small change in the oscillator strengths of fundamental resonances of a medium, the appearance of new resonances related to impurities) can noticeably change the dispersion $\delta_{o,e}(\lambda)$ of the crystal. Concentration dependences

$\delta_{o,e}(C_{Mg})$ at fixed wavelengths λ also give information on variation in the dynamic parameters of the crystal and the type of rearrangement of structural defects.

Based on the oscillator model, the dispersion $n^2(\lambda)$ in the transparency region (both for o-polarised and e-polarised waves; in this section, we omit for brevity a pair of polarisation indices at all coefficients) can be written in the form

$$n^2(\lambda) = A_{UV} + \sum_{i_{el}} \frac{A_{i_{el}}}{\lambda_{i_{el}}^{-2} - \lambda^{-2}} + \sum_{i_{ph}} \frac{A_{i_{ph}}}{\lambda_{i_{ph}}^{-2} - \lambda^{-2}}, \qquad (2)$$

where the term A_{UV} is the plasmon contribution in the far UV region. Summation in the second term is performed over all oscillators i_{el} describing the contribution from electronic excitations, and summation in the third term is performed over all dipole-active phonon modes i_{ph}.

The coefficients $A_{i_{ph}}$ and $\lambda_{i_{ph}}$ are the oscillator strengths and resonance phonon wavelengths, respectively, and the coefficients $A_{i_{el}}$ and $\lambda_{i_{el}}$ are the corresponding quantities for electron resonances. Both the electron and phonon resonances can be assigned to certain ions of a crystal lattice: ions of an ideal crystal, structural defects of a pure crystal, or doping ions. In the simplest approximation, the intrinsic wavelengths are independent of the concentration, whereas all the oscillator are proportional to concentrations of the corresponding ions: $A_{i_{ph,el}} = a_{i_{ph,el}} C_i$.

As a rule, the contributions from impurity ions and structural defects to the expression for the total permittivity (2) are negligibly small. However, the difference between (2) and the similar dependence for the undoped crystal does not contain the contribution from ions whose concentration does not change upon variation of the doping degree. For this reason, the oscillating dependence of $\delta(\lambda)$ contain only the terms with the oscillator strengths depending on the impurity concentration.

According to the existing crystallographic models [11–13], doping of $LiNbO_3$ with Mg ions can change concentrations of Li and Nb ions located in sites of the ideal crystal (Li_{Li} and Nb_{Nb}), concentrations of Nb ions located in the Li sites (Nb_{Li}) and of Mg ions located in the Li sites (Mg_{Li}) or in the Nb sites (Mg_{Nb}). This means that the expression for $\delta(C_{Mg},\lambda)$ can be represented in the form

$$\delta(C_{Mg},\lambda) = f_{Mg_{Li}}(\lambda) C_{Mg_{Li}}(C_{Mg}) + f_{Mg_{Nb}}(\lambda) C_{Mg_{Nb}}(C_{Mg})$$

$$+ f_{Nb_{Li}}(\lambda)\left[C_{Nb_{Li}}(C_{Mg}) - C_{Nb_{Li}}(0)\right] + f_{Li_{Li}}(\lambda)\left[C_{Li_{Li}}(C_{Mg}) \right. \qquad (3)$$

$$\left. - C_{Li_{Li}}(0)\right] + f_{Nb_{Nb}}(\lambda)\left[C_{Nb_{Nb}}(C_{Mg}) - C_{Nb_{Nb}}(0)\right],$$

where

$$f_j(\lambda) = \sum_{i_{el}^j} \frac{a_{i_{el}^j}}{\lambda_{i_{el}^j}^{-2} - \lambda^{-2}} + \sum_{i_{ph}^j} \frac{a_{i_{ph}^j}}{\lambda_{i_{ph}^j}^{-2} - \lambda^{-2}}; \qquad (4)$$

$j = Li_{Li}, Nb_{Nb}, Nb_{Li}, Mg_{Li}, Mg_{Nb}$; C_j are the concentrations of the corresponding ions; subscripts i_{el}^j and i_{ph}^j refer to the electron and lattice modes involving jth ions.

Thus, a study of the dispersion dependences $\delta(\lambda)$ of crystals containing Mg ions at different concentrations allows us to analyse a variation in the parameters of weak resonances with intrinsic wavelengths $\lambda_{i_{el}^j}$ and $\lambda_{i_{ph}^j}$, and a study of dependences $\delta(C_{Mg})$ at fixed wavelengths in different frequency regions gives information on a change in the defect concentration and the doping mechanism.

Coefficients of the type $C_j(C_{Mg}) - C_j(0)$ in (3), which depend on the concentration, can increase with the concentration of Mg if the number of ions of a given type increases, or they can decrease if these ions set free the corresponding lattice sites. When the dispersion $n^2(\lambda)$ of the medium is positive, the oscillator strengths $A_{i_{ph,el}}$ and corresponding proportionality coefficients $a_{i_{ph,el}^j}$ are positive.

Thus, if the concentration of ions of some type increases with increasing doping degree, the corresponding contribution to $\delta(C_{Mg})$ from phonon excitations in the region $\lambda_{i_{el}} < \lambda < \lambda_{i_{ph}}$ should result in the decrease in $\delta(C_{Mg})$, while the contribution from the electron UV resonances should increase $\delta(C_{Mg})$ upon doping. If the ion concentration in the corresponding sites decreases, the situation is reversed: the IR vibrational modes cause an increase in $\delta(C_{Mg})$, while the UV resonances lead to its decrease. The total picture in the general case is a sum of several such processes, the relation between the contributions from each process being dependent on the observation wavelength.

We did not take into account the additional resonances that can appear in the transparency region of a crystal. Being only weakly noticeable against the dispersion of the total response of the medium (2), such resonances can be observed in difference spectra $\delta(\lambda)$.

3.1. Dispersion dependences $\delta_o(\lambda)$ of crystals with different Mg concentrations

Fig. 1 summarise the results of measurements of the dispersion dependences $\delta_o(\lambda)$ of crystals containing different amounts of Mg in the visible and IR spectral regions. Note some curves are nonmonotonic in the spectral regions from 1 to 2 μm and from 2.8 to 3.5 μm. A change in the slope of the dispersion curves in the region between 2.8 and 3.5 μm is observed for all doped crystals, whereas in the region

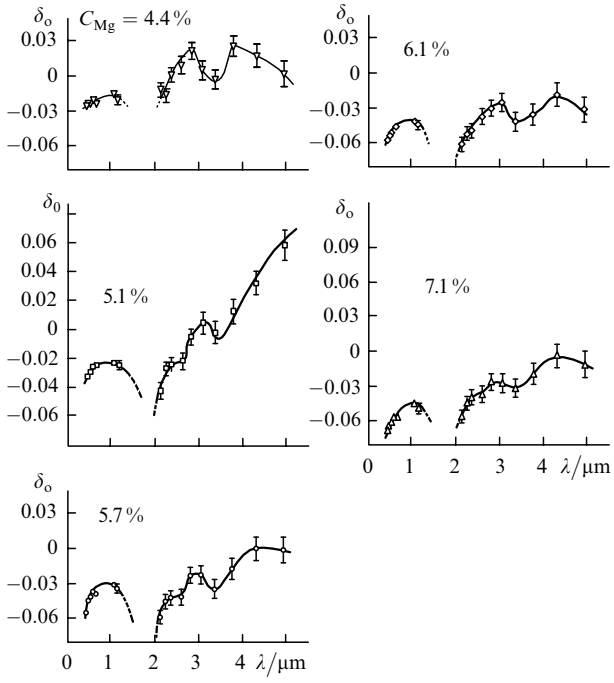

Figure 1. Dispersion $\delta_o = n_o^2(C_{Mg},\lambda) - n_o^2(0,\lambda)$ for $LiNbO_3$ at different concentrations of the Mg dopant.

between 1 and 2 μm, this change is observed only for the crystals with high impurity concentration and is absent for crystals with $C_{Mg} < 5.1\,\%$. Unfortunately, there is no experimental points in the spectral ranges from 0.6 to 1 μm and from 1.25 to 2 μm in Fig. 1, however, the resonance behaviour is confirmed by the type of the dependence $\delta_o(\lambda)$ in boundary regions.

The resonance behaviour found in the region between 1 and 2 μm is consistent with the measurements of absorption induced in lithium niobate crystals upon their chemical reduction, x-ray irradiation, or two-photon absorption [5, 13–17]. The one-photon absorption spectra of such crystals exhibit broad bands at $\lambda \sim 0.5$ and ~ 0.76 μm. If the Mg concentration exceeds the threshold concentration C_{th}, a new band appears at $\lambda \sim 1.2$ μm.

The threshold Mg concentration is defined as the concentration C_{th} above which photorefraction is almost completely suppressed, whereas at $C_{Mg} < C_{th}$, a crystal still possesses weak photorefractive properties. According to Ref. [16], photorefractive properties of nominally pure lithium niobate with a nonstoichiometric composition are related to Nb ions occupying Li vacancies (Nb_{Li}). According to most of the modern models of the defect structure of lithium niobate and the mechanisms of its doping [11–13, 16], the Mg ions gradually substitute the Nb ions in Li vacancies with increasing the Mg concentration in the region $C_{Mg} < C_{th}$. At $C_{Mg} = C_{th}$, all the Nb_{Li} defects disappear and the crystal loses its photorefractive properties.

The 0.76-μm absorption band is assigned to small-radius polarons, which are localised at structural defects Nb_{Li} [13], the 0.5-μm band is assigned to bipolarons localised at neighbouring Nb_{Li} and Nb_{Nb} ions [13, 16]. Both these bands should disappear, together with Nb_{Li}, when C_{Mg} exceeds the threshold concentration C_{th}. In Ref. [16], the 1.2-μm absorption band, which appears when $C_{Mg} > C_{th}$, was assigned to polarons localised at Nb_{Nb} ions.

Our measurements showed that spectra of the real part of the permittivity exhibit resonances in the region from 1 to 2 μm, whose concentration dependence is the same as that for the above absorption bands. In this region, the dispersion curve $\delta_o(\lambda)$ of crystals with the impurity concentration $C_{Mg} = 4.4\,\%$ is almost horizontal, and the behaviour of the other curves can be explained by assuming the presence of a deep minimum of the dispersion curve. A general form of the dispersion curves of crystals with the impurity concentration exceeding C_{th} indicates to the presence of a broad resonance band.

It seems likely that a weaker resonance band is also present in the spectrum of a crystal with [Mg] below the threshold concentration. If it is the same polaron resonance that was earlier observed in the absorption spectra of reduced or irradiated crystals [17], then the resonance behaviour of $\delta_o(C_{Mg},\lambda)$ should be observed because of the presence of a resonance band in the spectrum of a doped crystal rather than because of the specific features of the dispersion dependence $n_o^2(0,\lambda)$ of a nominally pure crystal.

According to the experimental data, the dependence $\delta_o(C_{Mg},\lambda)$ in the resonance region is negative. This means that the corresponding resonance of the permittivity of a $Mg:LiNbO_3$ crystal is also negative.

The nature of the band observed in the region between 2.8 and 3.5 μm is still unknown. It has been shown [13, 15, 16] that the absorption spectra changed qualitatively in the region of vibrations of OH groups upon variation of C_{Mg} in the near-threshold region. However, the observed bands are substantially broader than phonon resonances and they do not change qualitatively after passage through C_{th}.

3.2. Concentration dependences $\delta_o(C_{Mg})$ and $\delta_e(C_{Mg})$ in the visible range

Figs 2 and 3 show concentration dependences $\delta_o(C_{Mg})$ and $\delta_e(C_{Mg})$ at different wavelengths in the visible spectral range. The dashed lines represent analytic dependences calculated by the generalised Sellmeyer formula suggested in Ref. [18]. The authors of Ref. [18] derived a generalised formula based on their own measurements of the dispersion of crystals containing Mg ions at different concentrations and on a simplified model of structural changes caused by doping.

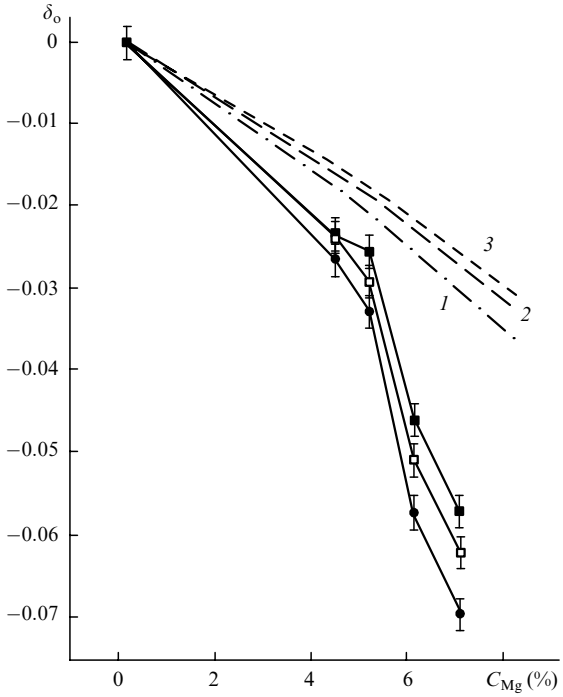

Figure 2. Measured (circles and squares) and calculated by the generalised Sellmeyer formula [18] (dashed and dashed-dotted lines) dependences of δ_o on the Mg concentration in $LiNbO_3$ for $\lambda = 0.4358$ (●, *1*), 0.532 (□, *2*), and 0.6328 μm (■, *3*).

The calculation was performed assuming that an undoped $LiNbO_3$ crystal has vacancies only in sites of the Li lattice. As the Mg concentration increases in the region below the threshold ($C_{Mg} < C_{th}$), the impurity ions displace Nb_{Li} ions. This is accompanied by a proportional increase in the oscillator strength of the electron resonance related to Mg_{Li}, whereas the oscillator strength of the resonance related to Nb_{Li} linearly decreases and becomes zero when the threshold concentration C_{th} is achieved. At the second stage, when $C_{Mg} > C_{th}$, only the electron resonance related to Mg_{Li} contributes to $\delta_{o,e}(C_{Mg})$. This contribution continues to grow proportionally to C_{Mg}. The model does not take into account possible changes in the Nb sites, as well as variation in the Li_{Li} concentration. This model yields a piecewise linear dependence $\delta_{o,e}(C_{Mg})$ with the only kink at the point $C_{Mg} = C_{th}$.

One can see from Fig. 2 that the curves for o-polarised electromagnetic radiation are in good qualitative agreement with the theoretical dependences obtained using the generalised Sellmeyer formula. The slope of the linear dependences

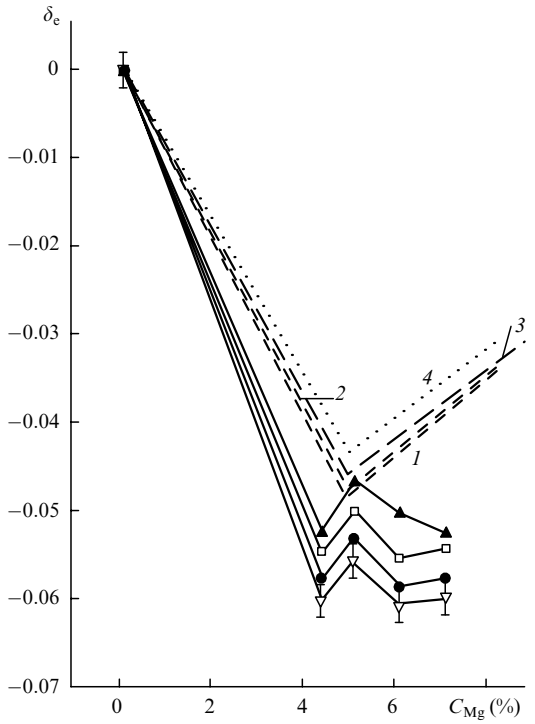

Figure 3. Measured (circles, triangles, and squares) and calculated by the generalised Sellmeyer formula [18] (dashed and dotted lines) dependences of $\delta_e = n_e^2(C_{Mg},\lambda) - n_e^2(0,\lambda)$ on the Mg concentration in $LiNbO_3$ for $\lambda =$ 0.4765 (▽, *1*), 0.4965 (●, *2*), 0.532 (□, *3*), and 0.6328 μm (▲, *4*).

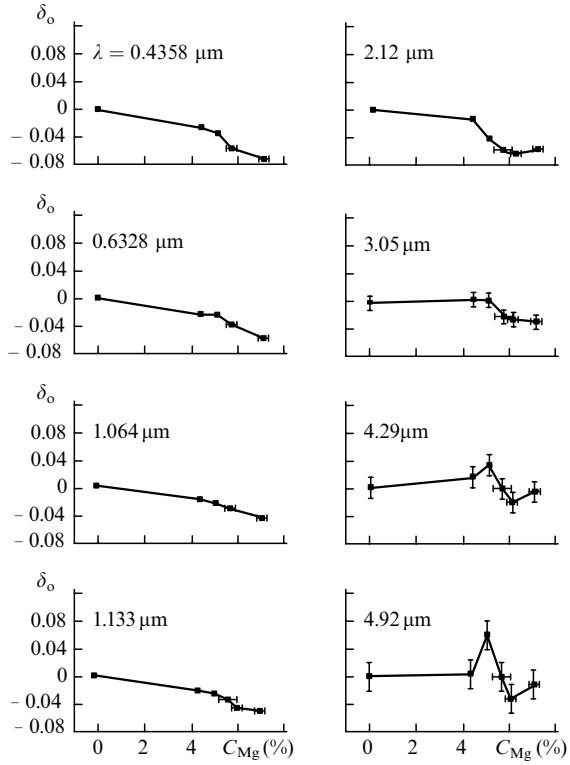

Figure 4. Dependences of δ_o on the Mg concentration in $LiNbO_3$ for different wavelengths in the visible and IR spectral regions.

of the ordinary refractive index occurs at the concentration $C_{Mg} \approx 5\%$, which was determined in Ref. [18] as the threshold concentration C_{th} for a congruent crystal. The deviation of the experimental data from the calculations is, in principle, within the total experimental error, which was 1.3×10^{-3} for measurements of $n_{o,e}$ [18]. However, in the case of the extraordinary refractive index, our data even qualitatively strongly deviate from the calculations. One can see from Fig. 3 that our dependences have at least two, and in the short-wavelength region, three kinks in which the slope of the curve changes.

3.3. Concentration dependences $\delta_o(C_{Mg})$ in the IR range

Fig. 4 shows the concentration dependences for $\delta_o(C_{Mg})$ for o-polarised waves in different parts of the transparency region of the crystal. For comparison, two typical concentration dependences $\delta_o(C_{Mg})$ in the visible range are also shown. One can see that dependences $\delta_o(C_{Mg})$ become more complicated with increasing wavelength. Beginning from $\lambda \simeq 4$ μm, the function $\delta_o(C_{Mg})$ exhibits three kinks. In the visible range, the four-step character of dependences $\delta_e(C_{Mg})$ for e-polarised waves is manifested upon approaching the UV resonances of the medium (Fig. 3). In the IR part of the transparency region, the function $\delta_o(C_{Mg})$ changes in the same wave upon approaching IR resonances.

It is clear that the change in concentration dependences $\delta_o(C_{Mg})$ with increasing wavelength in the IR region is caused by the enhancement of the influence of polar phonons. In the visible and near-IR regions, the slopes of the straight lines at different intervals of the dependence $\delta_o(C_{Mg})$ can differ only weakly, and the measurement error of refractive indices (although being lower in magnitude than that in the long-wavelength IR region) can prevent the observation of three distinct kinks in these dependences.

4. Structural transformations caused by doping with Mg

Let us discuss the possible types of structural transformations at the four stages of variation of C_{Mg}: in the regions $C_{Mg} < 4.4\%$, $4.4 < C_{Mg} < 5\%$, $5 < C_{Mg} < 6\%$, and $C_{Mg} > 6\%$. The dispersion of the refractive index in the visible region is mainly affected by the nearest electron resonances related to the Nb_{Nb}, Nb_{Li}, Mg_{Nb}, and Mg_{Li} ions [18, 19]. The nearest resonances in the IR transparency region of the crystal are vibrational modes of the NbO_3 octahedron with frequencies in the region from 230 to 880 cm^{-1} [20]. Vibrations of the Li_{Li}, Nb_{Li}, and Mg_{Li} ions relative to their oxygen environment have substantially lower frequencies, which lie below 200 cm^{-1} [21]. Nevertheless, it is the Li – O vibration of the E type with the transverse frequency equal to 152 cm^{-1} that has the maximum oscillator strength [20], and the influence of the ions located at the Li sites on the dispersion of the ordinary refractive index of the crystal in the IR transparency region cannot be neglected.

Let us analyse the observed concentration dependences from the point of view of the four-stage model of structural ransformations proposed in Ref. [12].

(1) According to this model, structural transformations can be described at the first stage by the reaction (in the Kröger – Vink notation)

$$5MgO + 3\left(Nb_{Li}^{4\cdot}V_{Nb}^{5\prime}\right) + 2Nb_{Li}^{4\cdot} \leftrightarrow 5Mg_{Li}^{\cdot} + Nb_2O_5\,. \quad (5)$$

In this case, the Nb_{Li} concentration decreases and the Mg_{Li} concentration increases. The dispersion in the visible range was calculated in Ref. [18] assuming that that the same variations occurred at the first stage. It seems likely that the same structural transformations determine the decrease in

$\delta_{o,e}(C_{Mg})$, which we observed in the region $C_{Mg} < 4.4\,\%$. This means that the decrease in the Nb_{Li} concentration affects the dispersion in the visible region in a greater degree than the increase in the Mg_{Li} concentration. No change in the refractive index in the IR region was observed at this stage. This means that a change in the total phonon contribution with decreasing Nb_{Li} concentration and increasing Mg_{Li} concentration is negligible.

(2) At the second stage, structural transformations are described by the reaction

$$5MgO + 4\left(Nb_{Li}^{4\cdot}V_{Nb}^{5\prime}\right) + Nb_{Li}^{4\cdot} \leftrightarrow 5Mg_{Li}^{\cdot} + 5V_{Li}^{\prime} + LiNbO_3 + 2Li_2O \quad (6)$$

or by the close reaction

$$MgO + \left(Nb_{Li}^{4\cdot}V_{Nb}^{5\prime}\right) \leftrightarrow Mg_{Li}^{\cdot} + 2V_{Li}^{\prime} + Li_2O\,. \quad (7)$$

This means that the Nb_{Li} and Mg_{Li} concentrations continue to decrease and increase, respectively, with the same rates, and also the escape of Li_{Li} ions occupying their sites in a lattice occurs.

These changes are consistent with an increase in $\delta_o(C_{Mg})$ in the IR region for $4.4\% < C_{Mg} < 5\,\%$ and also with the fact that dependences $\delta_o(C_{Mg})$ in the visible region do not change their character within this concentration range because electron resonances of Li_{Li} are remote. Nevertheless, dependences $\delta_e(C_{Mg})$ also exhibit a rise in the visible region in the above concentration range. Because this rise does not increase substantially upon approaching the UV boundary of the transparency region, it can be also explained by the influence of phonon resonances.

However, phonon resonances related to vibrational modes of Li_{Li} are too remote from the transparency region to produce such effect. If we attempt to explain dependences $\delta_e(C_{Mg})$ in the visible region by variations in the oscillator strengths of the electron subsystem, we should assume the presence of some additional changes in the concentrations of Nb_{Nb}, Nb_{Li}, Mg_{Li}, and Mg_{Nb} ions.

It was assumed in Ref. [16] that Nb_{Nb} vacancies in Zn : $LiNbO_3$ crystals can be occupied by Zn_{Nb} ions in the concentration range below the threshold concentration. Let us assume that the process

$$4MgO + 4\left(Nb_{Li}^{4\cdot}V_{Nb}^{5\prime}\right) + Nb_{Li}^{4\cdot} \leftrightarrow 3Mg_{Li}^{\cdot} + Mg_{Li}^{3\prime} + LiNbO_3 + Li_2O. \quad (8)$$

occurs in Mg : $LiNbO_3$ for $4.4\% < C_{Mg} < 5\,\%$.

In this case, along with decreasing Li_{Li} concentration, the Mg_{Nb} concentration increases. This can result in the increase in $\delta_e(C_{Mg})$ in the visible spectral region.

(3) Structural transformations at the third stage, above the threshold concentration $C_{th} = 5\,\%$, were described in Ref. [12] by the reaction

$$3MgO + V_{Li}^{\prime} \leftrightarrow 2Mg_{Li}^{\cdot} + Mg_{Nb}^{3\prime} + LiNbO_3, \quad (9)$$

i. e., processes caused by the decrease in the Nb_{Li} concentration cease, the Mg_{Li} concentration continues to increase, the Mg_{Nb} concentration also increases, and both Li_{Li} and Nb_{Nb} are released. The transformations are so diverse that they can be successfully matched with any variations in the refractive index both in the IR and visible regions. To do this, it is sufficient to assume that one or another of the resonances predominantly affects $\delta_{o,e}(C_{Mg})$. Note that this assumption will be less stringent, if we assume that structural transformations at the previous stage occurred according to reaction (8), i. e., the Mg ions already began to occupy vacant Nb sites.

(4) It is assumed that the following process takes place at the fourth stage:

$$4MgO \leftrightarrow 3Mg_{Li}^{\cdot} + Mg_{Nb}^{3\prime} + LiNbO_3 + Li_2O. \quad (10)$$

This process differs from the third-stage process by the increase in the rate of release of Li_{Li} ions. As would be expected, in this case, variations in the visible range are virtually unnoticeable and the abrupt decrease of $\delta_o(C_{Mg})$ in the IR range ceases.

Thus, the above experimental dependences show the presence of four stages of structural transformations. These dependences qualitatively agree with models [12, 16] and allow one to determine the Mg concentration at which mechanisms of the impurity incorporation into a crystal change.

5. Conclusions

We have measured dispersions of the ordinary and extraordinary refractive indices of congruent Mg : $LiNbO_3$ crystals in the visible spectral region with an absolute error of ± 0.0002 and the dispersion of the ordinary refractive index in ranges from 1 to 1.25 μm and from 2 to 3 μm with an error of ± 0.0005, in the range between 3 and 4 μm with an error of no worse than ± 0.001, and in the range from 4 to 5 μm with an error of about ± 0.002. These data can be used in calculations of frequency doublers and optical parametric transducers in a broad frequency range.

We have studied the influence of the Mg impurity on the optical parameters and the structure of lithium niobate from the dispersion and concentration dependences of the difference $\delta_{o,e}(C_{Mg},\lambda) \equiv n_{o,e}^2(C_{Mg},\lambda) - n_{o,e}^2(0,\lambda)$ characterising the difference between the real parts of permittivities of doped and undoped crystals in the transparency region. Analysis of the concentration dependences of $\delta_{o,e}(C_{Mg})$ in the visible and IR regions based on the oscillator model of the dispersion $n_{o,e}^2(\lambda)$ is indicative of the four-stage mechanism of the Mg impurity incorporation into a $LiNbO_3$ crystal lattice in the range $C_{Mg} \leqslant 7\,\%$.

Our experimental data qua-litatively agree with the model developed in Ref. [12]. According to this model, along with the changes in structural transformations taking place at the threshold Mg concentration, the mechanisms also change both in the region below and above the threshold concentration. These changes are caused first of all by the dynamics of the Li_{Li} concentration. When considering the structural transformations occurring at the second stage (below the threshold), it is appropriate to take into account also the possible initial occupation of the Nb sites by Mg ions according to a scheme proposed in Ref. [16].

The dispersion dependences $\delta_o(\lambda)$ of crystals in the transparency region exhibit resonances in the ranges from 1 to 2 μm and from 2.8 to 3.5 μm. The resonance in the range between 1 and 2 μm is strongly enhanced in crystals containing Mg at a concentration above 5.1 %. The dependence of this resonance on the impurity concentration is similar to that of the polaron absorption band in samples subjected to x-ray irradiation or chemical reduction [17]

Acknowledgements. The authors thank S V Lavrishchev and V N Talonova for independent x-ray analysis of the Mg impurity in samples, A A Mikhailovskii for his great help in the study, T R Volk and A V Shepelev for useful comments and discussions of the results. This work was supported by the 'Integration: Fundamental Optics and Spectroscopy' program and the Russian Foundation for Basic Research (Grants Nos. 99-02-16418 and 98-02-16877).

References

1. Byer R L *J. Nonlin. Opt. Phys. Mater.* **6** 549 (1997)
2. Glass A M *Science* **222** 657 (1984)
3. Tao S, Selviah D R, Midwinter J E *Opt. Lett.* **18** 912 (1993)
4. Abrahams S C, Marsh P *Acta Cryst. B* **42** 61 (1986)
5. Donnerberg H, Tomlinson S M, Catlow C R A, Schirmer O F *Phys. Rev. B* **40** 11909 (1989)
6. Volk T, Wohlecke M, Rubinina N, Reichert A, Razumovsky N *Ferroelectrics* **183** 291 (1996)
7. Amodei J J, Phillips W, Staebler D L *Appl. Opt.* **11** 390 (1972)
8. Wohlecke M, Gorradi G, Betzler K *Appl. Phys. B* **63** 323 (1996)
9. Aleksandrovskii A L, Ershova G I, Kitaeva G Kh, Kulik S P, Naumova I I *Kvantovaya Elektron. (Moscow)* **18** 254 (1991) [*Sov. J. Quantum Electron.* **21** 225 (1991)]
10. Kitaeva G Kh, Naumova I I, Mikhailovsky A A Losevsky P S, Penin A N *Appl. Phys. B* **66** 201 (1998)
11. Qiren Z, Xiqi F *Phys. Rev. B* **43** 12019 (1992)
12. Donnerberg H, Tomlinson S M, Catlow C R A, Schirmer O F *Phys. Rev. B* **44** 4877 (1991)
13. Schirmer O F, Thiemann O, Wohlecke M *J. Phys. Chem. Solids* **52** 185 (1991)
14. Schirmer O F, von der Linde *Appl. Phys. Lett.* **33** 35 (1978)
15. Volk T R, Rubinina N M *Fiz. Tverd. Tela{w* **33** 1192 (1991)
16. Volk T, Rubinina N, Wohlecke M *J. Opt. Soc. Am. B: Opt. Phys.* **11** 1681 (1994)
17. Sweeney K L, Halliburton L E, Bryan D A, Rice R R, Gerson R, Tomaschke H E *J. Appl. Phys.* **57** 1036 (1985)
18. Shlarb U, Betzler K *Phys. Rev. B* **50** 751 (1994)
19. Shlarb U, Betzler K *Phys. Rev. B* **48** 15613 (1993)
20. Barker A S, Loudon R *Phys. Rev.* **158** 433 (1967)
21. Hu L J, Chang Y H, Chang C S, Yang S J, Hu M L, Tse W S *Mod. Phys. Lett. B* **5** 789 (1991)